International Journal of Agriculture and Biosciences 2026 15(2): 772-781.
https://doi.org/10.47278/journal.ijab/2025.226

RESEARCH ARTICLE
eISSN: 2306-3599; pISSN: 2305-6622

# Green-Synthesized Silver Nanoparticles as Antifungal Agents against Tomato Vascular Wilt

Rebhi Darwazah[1], Nidá Salem [1]* and Akl Awwad[2]

[1]The University of Jordan, School of Agriculture, Department of Plant Protection, Amman 11942, Jordan
[2]Royal Scientific Society, Department of Materials Science, Amman 11941, Jordan
*Corresponding author: n.salem@ju.edu.jo

## ABSTRACT

Tomato (*Solanum lycopersicum*) is a globally important crop that faces significant yield losses due to vascular wilt caused by *Fusarium oxysporum* f.sp. *lycopersici* (FOL), a persistent soil-borne pathogen. Conventional chemical fungicides used to combat this disease often pose environmental hazards and contribute to pathogen resistance, highlighting the urgent need for sustainable alternatives. This study aimed to explore the antifungal potential of silver nanoparticles (AgNPs) synthesized through a green approach using aqueous leaf extracts from *Eriobotrya japonica*, *Ficus carica* and *Olea europaea*. The synthesized AgNPs were characterized by X-ray Diffraction (XRD), UV-Visible Spectroscopy (UV-Vis), Scanning Electron Microscopy (SEM) and Energy Dispersive X-ray Spectroscopy (EDS). AgNPs that are synthesized from *E. japonica* were tested through both laboratory assays and greenhouse trial to assess their inhibitory effects on FOL growth and disease progression. Results demonstrated that AgNPs significantly suppressed fungal development. Treated tomato plants exhibited reduced wilt symptoms compared to untreated controls. The application of green-synthesized AgNPs showed variable effects on the growth and development of tomato plants (cv. Dafnes) under greenhouse conditions. These findings highlight the potential of green-synthesized AgNPs as an eco-friendly and effective strategy for managing Fusarium wilt in tomato crops. By integrating green nanotechnology with plant disease management, this approach offers a promising alternative to chemical fungicides, contributing to sustainable agriculture and improved crop protection.

**Keywords:** Nanoparticles; Fusarium wilt; Plant extract; Loquat.

**Article History**
Article # 25-545
Received: 12-Sep-25
Revised: 12-Nov-25
Accepted: 09-Dec-25
Online First: 25-Dec-25

## INTRODUCTION

Tomato (*Solanum lycopersicum*) is one of the most economically significant vegetable crops cultivated worldwide. In Jordan, tomato cultivation plays a central role in agricultural production, particularly in the Jordan Valley, which serves as the country's primary hub for year-round tomato farming due to its favorable climate and fertile soils (Hamaideh et al. 2024). The Jordan Valley, with its subtropical climate and access to irrigation, supports intensive tomato production across both open fields and greenhouse systems. According to the Jordanian Department of Statistics, tomato cultivation accounts for approximately 27.5% of the total vegetable area and contributes over 43% of total vegetable production (Hassan, 2020). The region's tomato yield has shown steady growth, increasing from 51.7tons/ha in 2008 to 59.8tons/ha in 2012, with recent estimates indicating average yields exceeding 119tons/ha in greenhouse systems (Hassan, 2020). However, this productivity is increasingly threatened by soil-borne pathogens, particularly *Fusarium oxysporum* f. sp. *lycopersici* (FOL), the causal agent of Fusarium wilt. Fusarium wilt is a devastating vascular disease that affects tomato plants at all growth stages. The pathogen invades the root system, colonizes the xylem vessels, and disrupts water transport, leading to wilting, chlorosis, stunting, and eventual plant death (Heikal et al. 2025). In Jordan, FOL is considered one of the most prevalent and damaging tomato diseases, with races 1 and 2 being the most commonly reported (Al-Khatib et al. 2004). Yield losses due to Fusarium wilt in tomato can range from 30% to 40% globally, and in severely infested fields, losses may exceed

**Cite this Article as:** Darwazah R, Salem N and Awwad A, 2026. Green-Synthesized silver nanoparticles as antifungal agents against tomato vascular wilt. International Journal of Agriculture and Biosciences 15(2): 772-781. https://doi.org/10.47278/journal.ijab/2025.226

A Publication of Unique Scientific Publishers

50% (Hassan, 2020). The persistence of FOL in soil and its ability to survive as chlamydospores for extended periods make it particularly challenging to manage through conventional means.

Traditional management strategies for Fusarium wilt include crop rotation, soil solarization, chemical fungicides, and the use of resistant cultivars. However, these approaches have limitations. Chemical fungicides, while effective in the short term, pose risks to environmental health, contribute to pathogen resistance, and may leave harmful residues in produce (Haruna et al. 2024). Moreover, resistance breakdown due to emerging FOL races has been reported, necessitating alternative and more sustainable solutions (Pandey et al. 2024).

In recent years, integrated disease management (IDM) has gained prominence as a holistic approach to controlling Fusarium wilt. IDM combines cultural practices, biological control agents, resistant cultivars, and eco-friendly inputs to reduce disease pressure and enhance plant resilience (Choudhary et al. 2023). Among these innovations, nanotechnology has emerged as a promising tool in plant pathology. Specifically, silver nanoparticles (AgNPs) synthesized via green methods using plant extracts have demonstrated potent antifungal activity against a wide range of phytopathogens, including FOL (Kim et al. 2012; Devi & Bhimba, 2014; Narayanan & Park, 2014; Mahdizadeh et al. 2015; Wang et al. 2015; Abkhoo & Panjehkeh, 2016; Ahmad et al. 2022; Tabassum et al. 2024; Ashraf et al. 2025; Eker et al. 2025; El-Wafai et al. 2025). Green synthesis of AgNPs involves the use of plant-derived phytochemicals as reducing and stabilizing agents, offering an environmentally friendly alternative to chemical and physical nanoparticle production methods. Plant-mediated AgNPs are known for their biocompatibility, stability, and enhanced antimicrobial properties due to their small size and high surface area (Vanlalveni et al. 2021). Studies have shown that AgNPs disrupt fungal cell membranes, interfere with metabolic pathways, and inhibit spore germination, making them effective agents against soil-borne fungi (Mazhar et al. 2025).

In the context of tomato production in Jordan, the application of biosynthesized AgNPs offers a novel strategy for managing Fusarium wilt while minimizing environmental impact. The Jordan Valley, with its intensive tomato cultivation and vulnerability to soil-borne diseases, presents an ideal setting for evaluating the efficacy of green nanotechnology in disease suppression. Moreover, the integration of AgNPs into existing greenhouse systems aligns with national goals for sustainable agriculture and reduced chemical input (Hamaideh et al. 2024). This study investigates the green synthesis of AgNPs using aqueous leaf extracts from *Eriobotrya japonica* (loquat), *Ficus carica* (fig) and *Olea europaea* (olive), and evaluates their antifungal activity against FOL through both in vitro and in planta trials. These plant species were selected based on their known phytochemical profiles and local availability. The primary hypothesis is that loquat-mediated AgNPs, when applied at optimized doses, effectively suppress FOL while minimizing phytotoxicity in tomato plants. Secondary hypotheses include assessing the comparative performance of AgNPs relative to conventional fungicides and evaluating the antifungal effects of leaf extracts alone.

By exploring the potential of plant-mediated AgNPs, this research aims to advance the development of environmentally sustainable nanoparticle-based interventions for managing vascular wilt and enhancing tomato crop resilience in affected regions such as the Jordan Valley. The findings are expected to contribute to the growing body of knowledge on green nanotechnology in agriculture and support the transition toward safer, more sustainable plant protection strategies.

## MATERIALS & METHODS

### Synthesis and Characterization of AgNPs

$AgNO_3$ was procured from Aldrich Chemicals and used as the precursor for nanoparticle synthesis. Prior to experimentation, all glassware was thoroughly cleaned with sterile distilled water and dried in a hot-air oven to eliminate potential contaminants. The green synthesis of AgNPs was conducted following protocols previously established by Awwad et al. (2013, 2016). Aqueous leaf extracts were prepared by mixing 10g of dried leaf powder from *Eriobotrya japonica*, *Ficus carica* and *Olea europaea* with 400mL of distilled deionized water in a 500mL glass beaker. The mixture was boiled for 10 minutes until the color changed from clear to yellow or light brown, then cooled at room temperature (25 ± 2°C) for one hour. The cooled solution was filtered using Whatman No. 1 filter paper to remove residual biomaterials. The resulting extracts were stored at room temperature for further use. For nanoparticle synthesis, 5mL of each leaf extract was added to 100mLof 1 × $10^{-3}$M silver nitrate ($AgNO_3$) solution under continuous stirring with a magnetic stirrer. The reaction mixture was heated at 60°C for 10 minutes, during which the color changed to dark yellow-brown within one minute, indicating the formation of AgNPs. Black suspended particles were observed in the solution. The synthesized AgNPs were separated by centrifugation at 12,000rpm for 10 minutes, washed with ethanol, and dried in an oven at 60°C for 3 hours. The pH of the reaction mixture was maintained at approximately 6.5 during synthesis.

A schematic representation of the synthesis process using *E. japonica* extract is illustrated in Fig. 1.

The synthesized AgNPs were characterized using UV-Visible Spectroscopy (UV-Vis), X-ray Diffraction (XRD), Scanning Electron Microscopy (SEM) and Energy Dispersive X-ray Spectroscopy (EDS). UV-Vis spectra were recorded using a Shimadzu UV-1601 spectrophotometer (Shimadzu, Japan) and the surface plasmon resonance (SPR) peak was monitored to determine the λ_max of AgNPs. Crystallographic analysis was performed using an XRD-6000 diffractometer (Shimadzu, Japan) equipped with a Cu Kα radiation source (λ = 1.5406 Å), operated at 30kV and 30mA, with a Ni filter. Data were collected over a 2θ range of 3° to 80°, and peak indexing was carried out using standard JCPDS files. The average crystallite size of AgNPs was estimated using the Debye–Scherrer equation, assuming spherical particles and negligible strain. SEM and EDS analyses were conducted using a Quanta FEI 450 SEM system.

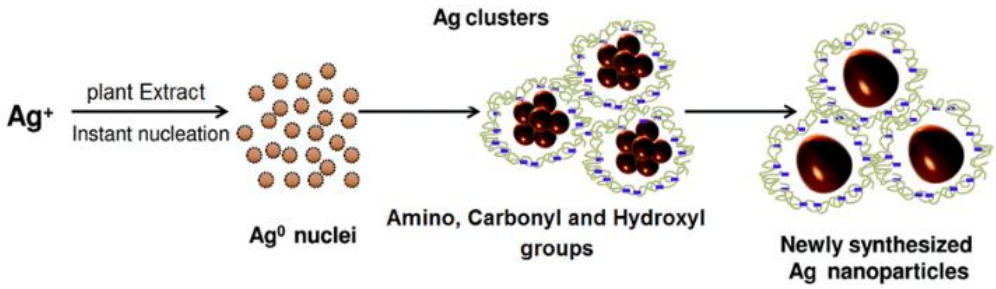


**Fig. 1:** Schematic illustration of the synthesis process of AgNPs using *Eriobotrya japonica* leaf extract.

Samples were mounted on aluminum stubs and sputter-coated with a 5-10nm layer of gold (Au or Au/Pd) using a laboratory coater, with coating times of approximately 30-60 seconds at moderate current, calibrated using witness samples. Imaging was performed at an accelerating voltage of 20kV. A drop of AgNP suspension was air-dried on the stub prior to coating and imaging.

**Fungal Isolate**

Tomato plants exhibiting wilting symptoms were sampled from crops cultivated under plastic house conditions in the Jordan Valley. Symptomatic plants were assessed for vascular discoloration in the stem tissues. Collected samples were placed in sterile plastic bags, transported to the laboratory under cooled conditions, and stored at 4°C until further analysis. Sections of discolored stem tissue were aseptically excised, surface-sterilized, and plated onto potato dextrose agar (PDA) plates and kept at 25°C for 10-14 days. Once the fungus has grown from the pieces, pure culture of fungus was prepared and identified based on morphological features using a diagnostic key (Leslie & Summerell, 2006). Microscopic examination of microconidia and macroconidia was performed using a Zeiss compound microscope (Oberkochen, Germany).

For molecular identification, genomic DNA was extracted from pure fungal culture using the I-genome BYF DNA Extraction Mini Kit (Zymo Research Corporation, Irvine, CA, USA), following the manufacturer's protocol. Molecular characterization was conducted by polymerase chain reaction (PCR) targeting the internal transcribed spacer (ITS) region and the translation elongation factor 1-alpha (TEF1-α) gene, using primer sets and protocols described by White et al. (1990) and O'Donnell et al. (1998), respectively. Amplified PCR products were purified and ligated into the pGEM-T Easy Vector (Promega, USA). Bidirectional sequencing of two clones representing ITS and TEF1-α was performed by Macrogen Inc. (Seoul, Korea), and the resulting sequences were submitted to the NCBI GenBank under accession numbers MT807046 and MT809754, respectively.

**Pathogenicity Test**

The pathogenicity of the fungal isolate was assessed through inoculation on tomato cultivar 'Dafnes' from Syngenta Seeds. A conidial suspension containing $8 \times 10^6$ conidia $mL^{-1}$ was prepared from a 14-day-old culture of the isolate grown on PDA. Tomato seedlings, aged two weeks, were gently uprooted, and their roots were trimmed before immersion in the conidial suspension for 30 minutes to facilitate infection. Subsequently, the treated seedlings were transplanted into pots containing sterilized soil, and an additional 50mL of the conidial suspension was applied directly to each pot. Plants were maintained under controlled greenhouse conditions, and symptom development was monitored over a 30-day period. To confirm the pathogenic role of the fungal isolate and fulfill Koch's postulates, the fungus was re-isolated from symptomatic plants exhibiting wilting. The recovered isolate was morphologically and molecularly compared to the original isolate, thereby validating its identity as the causal agent of disease. The confirmed fungal isolate, designated JO-FOL1, was subsequently employed in both in vitro and in planta assays.

Subcultures of the fungal isolate JO-FOL1, confirmed as FOL through both morphological characterization and molecular analysis, and validated via fulfillment of Koch's postulates, were cultivated on PDA plates. These cultures were subsequently employed in assays to evaluate the antifungal efficacy of biosynthesized AgNPs.

**In vitro Plate Assay**

AgNPs synthesized using aqueous leaf extract of *E. japonica* (loquat) were selected for antifungal activity assays due to their minimal particle diameter and optimal surface area-to-volume ratio, which are critical for enhanced bioactivity. A stock solution of AgNPs was prepared at a concentration of 255.2ppm and subsequently diluted to obtain working concentrations of 200ppm, 150ppm, 100ppm, 50ppm and 10ppm. PDA plates were subjected to different treatments (control, loquat extract, 10ppm, 50ppm, 100ppm, 150ppm and 200ppm concentrations of AgNPs) of 4 replicates. A one-cm diameter plug from the actively growing margin of the FOL isolate was transferred to the center of each PDA plate using a sterile corkborer. Plates were incubated at 25°C, and radial fungal growth was monitored daily. Measurements of colony diameter were recorded until the control plates exhibited complete coverage by fungal hyphae. Antifungal activity (percent of inhibition) was quantified using the Antifungal Index (AI), calculated according to the formula described by Aguilar-Mendez et al. (2011):

AI (%) = (1-D1/D2) X 100, where AI is the antifungal index, D1 is the colony diameter in the test dishes and D2 is the colony diameter in the control dish.

The in vitro assay experiment was repeated four times to confirm our results and ensure reproducibility. As no significant variation was observed among replicates, representative data from one experiment are presented herein.

**In planta Greenhouse Experiment**

This experiment was conducted in the greenhouse at the School of Agriculture (32.01141, 35.87283), the University of Jordan. Soil used for planting was sterilized by oven treatment at 80°C for 48 hours to eliminate any microbial contaminants. A total of 80 clean plastic pots (15cm diameter) were filled with a standardized soil mixture composed of clay loam, peat moss, and sand in a 1:1:1 ratio. The tomato cultivar 'Dafnes', commonly grown by farmers in the Jordan Valley, was selected for this study. Seeds were germinated in polystyrene seed trays and grown for 40 days prior to transplantation. The inoculum of FOL was prepared from two-week-old cultures grown on PDA plates at 25°C. Fungal hyphae and conidia were gently scraped from the surface of the culture and suspended in sterile distilled water. The suspension was homogenized thoroughly to ensure even distribution of conidia. Conidial viability was confirmed microscopically using a hemocytometer and trypan blue exclusion assay prior to inoculation. The conidial concentration was adjusted to $8 \times 10^6$ conidia $mL^{-1}$ using a hemocytometer, a density selected based on previous studies demonstrating effective and reproducible infection levels in tomato plants without causing excessive stress or non-specific damage (Jorge et at. 1992; Steinkellner et al. 2008).

To facilitate infection, roots of tomato seedlings (approximately 5cm in length) were trimmed and immersed in the FOL suspension for 5 minutes. Seedlings were then transplanted into pre-labeled pots, each assigned to a specific treatment group. For FOL-inoculated treatments, 50mL of conidial suspension was added to each pot, while control treatments received 50mL of sterile distilled water. Following inoculation, 300mL of the designated treatment: green synthesized AgNPs, loquat leaf extract, commercial fungicide (Tachigaren), or distilled water was applied to each pot. Tomato plants were cultivated under controlled greenhouse conditions for a duration of four months. Plants were irrigated and fertilized as needed throughout the experiment. A balanced NPK fertilizer (20:20:20) was applied at three-week intervals, beginning two weeks after transplanting and continuing until the fourteenth week. The greenhouse environment was maintained under a 14-hour light/10-hour dark photoperiod (lights on from 06:00 to 20:00), with natural daylight supplemented by high-pressure sodium and LED lamps to ensure consistent illumination. Relative humidity was maintained between 60% and 70%, which is considered optimal for tomato growth and development. Environmental parameters, including temperature and humidity, were monitored regularly to ensure stable growing conditions. Disease progression was assessed periodically throughout the cultivation period. Disease incidence and severity of Fusarium wilt of tomato were calculated at the end of the greenhouse experiment. Disease incidence was calculated based on the number of FOL-inoculated tomato plants showing yellowing and wilting symptoms and confirmed by vascular discoloration. Disease severity was assessed according to the 0-5 scale (Arabyat, 2004).

**Statistical Analysis**

The in vitro plate assay experiment was conducted using a completely randomized design (CRD) comprising seven treatments, each replicated four times. For the in planta experiment, a CRD was also employed, consisting of eight treatments with ten replicates (pots) per treatment. The impact of various treatments on hyphal diameter and plant growth parameters was statistically evaluated using analysis of variance (ANOVA), implemented through the General Linear Model (GLM) procedure in SAS software (Version 9.1.3). Mean comparisons among treatments were conducted using Fisher's Least Significant Difference (LSD) test, with significance determined at a probability level of $P<0.05$.

## RESULTS & DISCUSSION

**Characterization of Synthesized AgNPs**

**X-ray Diffraction Analysis**

The crystalline size and structural characteristics of the synthesized AgNPs were analyzed using XRD. AgNPs produced using leaf extracts of *E. japonica*, *F. carica* and *O. europaea* exhibited distinct diffraction peaks in their XRD profiles, confirming successful synthesis. Four prominent peaks at 2θ values of 38.2°, 44.1°, 64.2° and 77.89° correspond to the (111), (200), (220) and (311) crystallographic planes, respectively. These reflections are indicative of a face-centered cubic (fcc) structure of elemental silver, consistent with standard data from the Joint Committee on Powder Diffraction Standards (JCPDS files no. 84-0713 and 04-0783). The observed broadening of Bragg's peaks further supports the nanoscale nature of the particles. Fig. 2 illustrates the XRD pattern of AgNPs synthesized using *E. japonica* leaf extract.

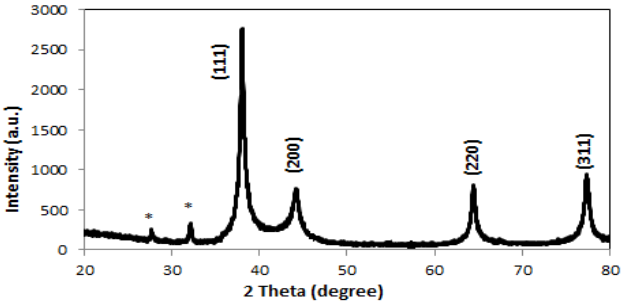


**Fig. 2:** X-ray diffraction (XRD) pattern of AgNPs synthesized using *Eriobotrya japonica* leaf extract.

The average particle size of AgNPs synthesized using leaf extracts of *E. japonica*, *F. carica* and *O. europaea* as both reducing and capping agents was estimated from XRD data using the Debye–Scherrer equation (Awwad et al. 2013). The calculated mean diameters of the AgNPs were 12.4nm, 24.72nm and 61.39nm for *E. japonica*, *F. carica* and *O. europaea*, respectively. Additionally, an unassigned diffraction peak (indicated by asterisks) was observed, which may suggest the presence of a bio-organic phase crystallized on the nanoparticle surface. Based on these findings, *E. japonica* leaf extract was selected for subsequent nanoparticle synthesis due to its production of the smallest particle size, offering a higher surface area-to-volume ratio and enhanced potential for biological applications.

### UV-Visible Spectroscopy Analysis

UV–Visible spectroscopy is widely recognized as one of the most employed techniques for characterizing nanoparticles. The synthesized AgNPs exhibited a distinct surface plasmon resonance (SPR) band within the wavelength range of 418–428nm, characteristic of silver (Fig. 3). These findings are consistent with those reported by Venkatesham et al. (2014), who observed a sharp SPR peak at 420nm in their UV–Vis analysis of AgNPs, further confirming the successful formation of AgNPs.

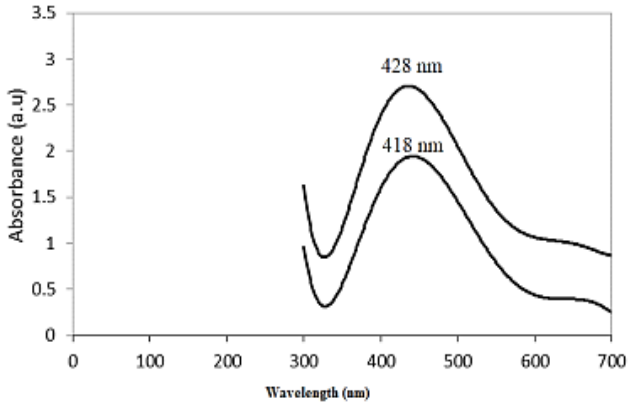


**Fig. 3:** UV-Vis spectrum showing the absorption of AgNPs synthesized by using *Eriobotrya japonica* leaf extract.

### Scanning Electron Microscopy (SEM) and Energy-Dispersive Spectroscopy (EDS) Analysis

The presence of AgNPs was confirmed through SEM and EDS. The SEM micrograph revealed well-defined, spherical particles and aggregated clusters, characteristic of AgNP morphology. Complementary EDS analysis (Fig. 4) provided elemental composition data, indicating a high silver content within the sample, with silver accounting for approximately 93.79% of the detected elements. These results collectively validate the successful synthesis and purity of the AgNPs.

### Anti-Fungal Activity of Silver Nanoparticles

### In vitro Plate Study

The antifungal efficacy of AgNPs against FOL was evaluated over a 9-day incubation period across varying concentrations. Fig. 5 illustrates the progression of fungal growth of the JO-FOL1 isolate over a 9-day period, following treatment with varying concentrations of AgNPs at 50, 100, 150 and 200ppm. These treatments were compared to FOL samples treated with loquat leaf extract and untreated control. Distinct differences in fungal growth patterns were observed across treatments during the one-week follow-up. Overall, a concentration-dependent inhibition of FOL growth was evident, with higher AgNP concentrations resulting in a marked reduction in hyphal diameter (Table 1).

**Table 1:** Inhibition rate (%) of silver nanoparticles against FOL on PDA media

| Treatment | Inhibition rate (%) * | | | |
|---|---|---|---|---|
| | Day 3 | Day 5 | Day 7 | Day 9 |
| 10ppm | 19.6$^{a}$ | 18.6$^{a}$ | 10.0$^{a}$ | 0.0$^{a}$ |
| 50ppm | 33.3$^{a}$ | 24.0$^{ab}$ | 10.9$^{a}$ | 3.9$^{ab}$ |
| 100ppm | 43.1$^{ab}$ | 33.3$^{bc}$ | 10.9$^{a}$ | 11.7$^{bc}$ |
| 150ppm | 43.1$^{ab}$ | 28.0$^{ab}$ | 30.9$^{b}$ | 15.6$^{c}$ |
| 200ppm | 68.0$^{b}$ | 44.0$^{c}$ | 29.1$^{b}$ | 15.6$^{c}$ |

Means followed by a different letter(s) in the same column differ significantly according to Fisher's least significant difference test (LSD); *Inhibition rates were determined based on four replicates (n = 4 plates per treatment).

On day 3, no statistically significant differences in inhibition were observed among the lower concentrations (10–150ppm), though the 200ppm treatment demonstrated a notably higher inhibition rate compared to 10ppm and 50ppm, suggesting the onset of a concentration-dependent response. By day 5, this trend became more distinct, with 200ppm showing significantly greater suppression of fungal growth than all other concentrations except 100ppm. The lack of consistent significance among intermediate concentrations (50–150ppm) indicates a nonlinear response in antifungal activity at early stages.

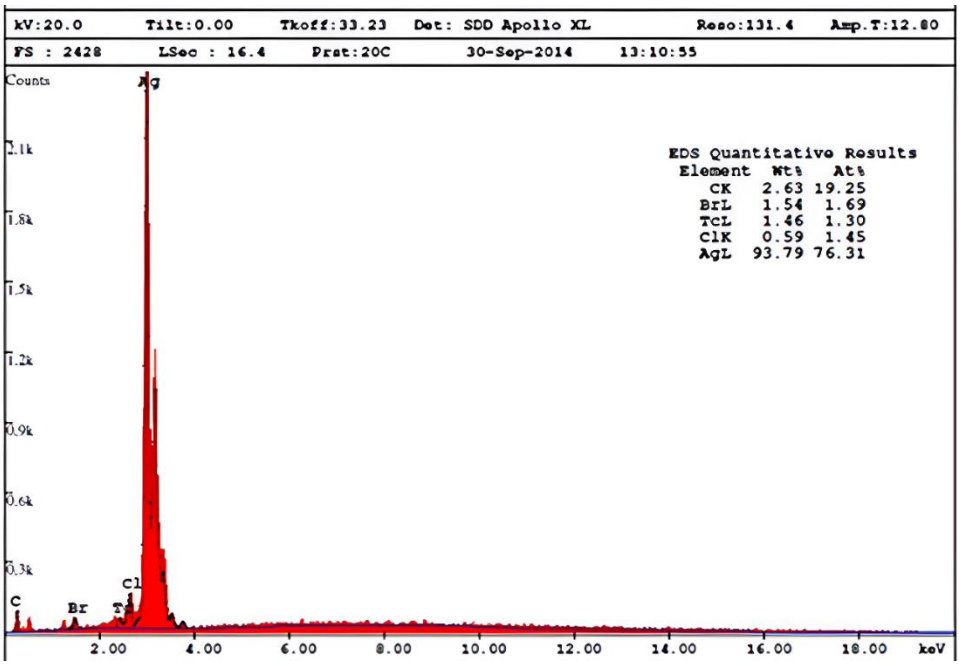


**Fig. 4:** Energy-dispersive X-ray spectroscopy (EDS) analysis of AgNPs synthesized using *Eriobotrya japonica* leaf extract.

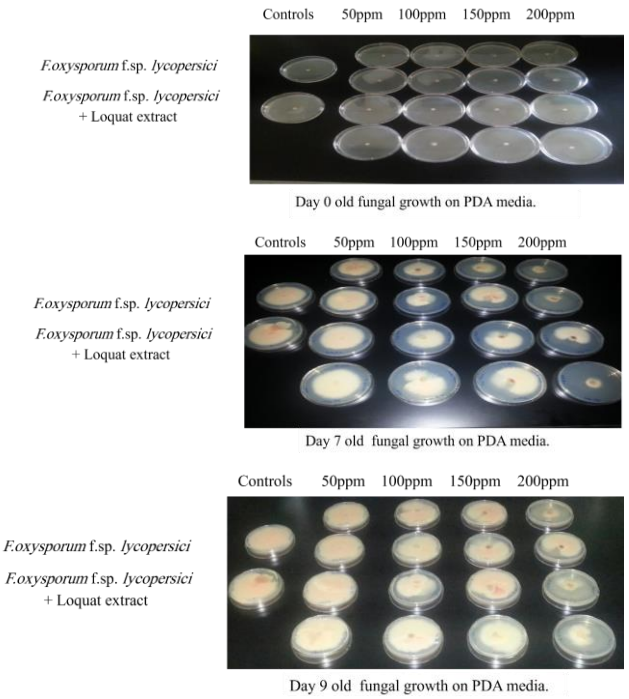


**Fig. 5:** Growth of FOL on PDA medium treated with AgNPs synthesized using *Eriobotrya japonica* leaf extract at concentrations of 50ppm, 100ppm, 150ppm and 200ppm, compared to untreated controls. Panels represent fungal development at different time points: (A) Day 0, (B) Day 7 and (C) Day 9 post-inoculation. n = 4 plates per treatment.

As incubation progressed to days 7 and 9, the inhibitory effects of higher concentrations became more pronounced. On day 7, both 150ppm and 200ppm treatments exhibited significantly greater inhibition than all lower concentrations, confirming their superior antifungal performance. By day 9, while 100ppm, 150ppm, and 200ppm treatments did not differ significantly from each other, they all showed markedly higher inhibition compared to 10ppm and 50ppm. These cumulative findings reinforce the concentration-dependent nature of AgNPs' antifungal activity, with 200ppm consistently yielding the highest suppression of FOL growth, and 10ppm the lowest, across all time points.

Overall, the data demonstrates that AgNPs effectively suppress the growth of FOL, and their antifungal activity increases with concentration. Additionally, the inhibition became more evident with longer incubation periods, suggesting that AgNPs may not only inhibit fungal growth but also delay its progression over time. Our findings are consistent with previous studies which highlighted the antifungal potential of nanoparticles, particularly AgNPs, against *Fusarium oxysporum* and other phytopathogenic fungi. The inhibitory effect of nanoparticles is often concentration-dependent, as demonstrated in research on zinc oxide nanoparticles (ZnONPs), where the highest inhibition rate was observed at 12ppm (Yehia & Ahmed, 2013). This trend mirrors the findings of the present study, reinforcing the idea that increased nanoparticle concentration enhances antifungal efficacy. AgNPs have shown strong antifungal activity even at low concentrations. For example, a concentration of 8µgmL$^{-1}$ was sufficient to suppress *F. oxysporum* growth significantly (Gopinath & Velusamy, 2013). AgNPs effectiveness is not limited to *Fusarium* species; they have also been reported to inhibit wood-degrading fungi such as *Gloeophyllum abietinum*, *G. trabeum*, *Chaetomium globosum* and *Phanerochaete sordida* (Narayanan et al. 2014), suggesting a broad-spectrum antifungal capability.

In agricultural applications, AgNPs have proven effective against powdery mildew in cucumbers and pumpkins. When applied both before and after disease onset, a concentration of 100ppm resulted in maximum inhibition of hyphal growth and conidial germination in vivo (Lamsal et al. 2011). This supports the potential of AgNPs as both preventive and curative agent in crop protection. Further evidence of AgNPs dose-dependent activity comes from in vitro experiments on *Neofusicoccum parvum*, a grapevine trunk disease pathogen. Increasing concentrations of AgNPs (2.5, 5, 10 and 40µgmL$^{-1}$) led to progressive inhibition of mycelial growth (Khatami et al. 2015). Kim et al. (2012) also showed dose-dependent inhibition of *F. oxysporum* at concentrations ranging from 10 to 100ppm. While silver remains the most extensively studied metal in nanoparticle form, other metallic nanoparticles have also shown promise. Copper nanoparticles (CuNPs), for instance, exhibited significant antifungal activity against *Phoma destructive*, *Curvularia lunata*, *Alternaria alternata* and *F. oxysporum* (Kanhed et al. 2014). This suggests that multiple types of nanoparticles could be harnessed for effective fungal control in agriculture.

Collectively, these studies underscore the potential of AgNPs as a powerful antifungal agent. Their consistent performance across various fungal species and experimental conditions supports their application in managing plant diseases, particularly when used at higher concentrations to maximize inhibition. Furthermore, the scanning electron microscopy (SEM) was employed to examine the morphological effects of AgNPs, synthesized using *E. japonica* (loquat) leaf extract, on the hyphal structure of FOL. The SEM analysis revealed noticeable structural alterations in the fungal hyphae treated with 200ppm AgNPs. Specifically, the treated hyphae exhibited a significant reduction in diameter (543nm) compared to the control hyphae (288µm), as illustrated in Fig. 6. This narrowing of the hyphal structure may contribute to impaired fungal growth and reduced pathogenicity. Similar morphological disruptions have been documented in previous studies. Choudhury et al. (2011) reported pronounced hyphal deformities in *F. oxysporum* following exposure to 200ppm sulfur nanoparticles (SNPs), supporting the findings of the present study. Das et al. (2015) observed that metallic nanoparticles such as $Mn^{2+}$, $Zn^{2+}$ and $Fe^{2+}$ at concentrations exceeding 200µgmL$^{-1}$, inhibited spore germination and altered the morphology of *Rhizopus oryzae* strain 1526. These results suggest that nanoparticle-induced structural damage is a common mechanism underlying fungal growth inhibition.

Further confirmation of the antifungal activity AgNPs comes from Kim et al. (2009), who demonstrated that AgNPs not only suppressed fungal proliferation but also caused hyphal tip breakage, conidial detachment and surface damage, ultimately leading to hyphal shrinkage. Medda et al. (2014) also reported similar effects using

AgNPs synthesized from *Aloe vera* leaf extract, which disrupted conidial germination and induced membrane deformation in *Rhizopus* and *Aspergillus* species, thereby inhibiting normal budding processes.

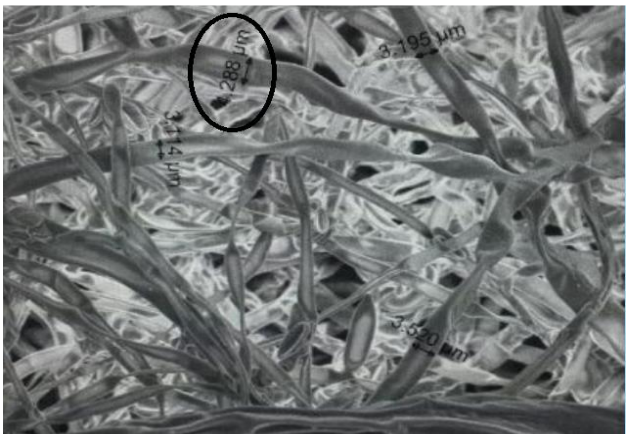


A

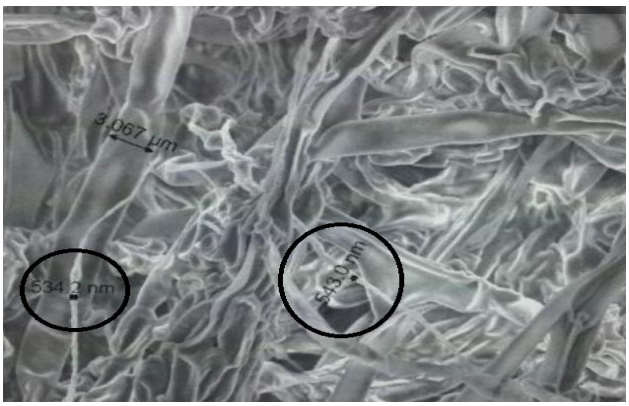


B

**Fig. 6:** SEM images of FOL: (A) untreated control showing normal hyphal morphology, and (B) sample treated with 200ppm AgNPs synthesized from *Eriobotrya japonica* leaf extract, exhibiting noticeable hyphal thinning (circled).

**In Planta Greenhouse Experiment**

Soaking the trimmed roots of tomato seedlings in FOL inoculum to aid infection caused a successful infection in treated tomato plants. This method aligns with the approach described by Cakır et al. (2014), who similarly achieved effective infection. Disease symptoms included yellowing and wilting of lower leaves, along with dark brown vascular discoloration. Fungal presence was subsequently confirmed by isolating the pathogen on PDA.

Fusarium wilt symptoms, as described by Miller et al. (1986), begin with slight vein clearing on the outer leaflets and drooping of leaf petioles. This is followed by progressive wilting and yellowing of the lower leaves, which eventually die before reaching maturity. In some cases, symptoms appear asymmetrically either affecting a single shoot or one side of the plant prior to full systemic infection.

To assess treatment efficacy, key growth parameters including stem diameter, and the fresh and dry biomass of shoots and roots were measured. Over a 15-week period, tomato plants subjected to various treatments including AgNPs, FOL-only, fungicide and loquat leaf extract exhibited dynamic changes in plant height (Table 2). At week 1, seedlings treated with 200ppm AgNPs combined with FOL (T1) showed significantly greater height than those under T3 (100ppm AgNPs + FOL), T5 (fungicide + FOL), and T7 (FOL-only control), suggesting stimulatory effect of high AgNPs concentration. However, by week 3, T1 displayed reduced growth compared to T4 (100ppm AgNPs), T5, and T6 (loquat extract + FOL), indicating a possible phytotoxic interaction between elevated AgNP levels and pathogen stress. These results align with Baskar et al. (2015), who reported growth inhibition in *Brassica rapa* ssp. *pekinensis* at AgNP concentrations of 250 and 500ppm, highlighting the dose-dependent nature of nanoparticle toxicity.

**Table 2:** Effect of AgNPs treatments on plant heights of tomato cv. Dafnes, grown under greenhouse conditions

| Treatment/Week | Plant heights* (cm) | | | | | | | |
|---|---|---|---|---|---|---|---|---|
| No. | 1 | 3 | 5 | 7 | 9 | 11 | 13 | 15 |
| T1 (200ppm + FOL) | $7.8^{ab}$ | $11.5^{b}$ | $16.4^{b}$ | $26.0^{b}$ | $43.0^{c}$ | $50.7^{b}$ | $61.1^{b}$ | $63.0^{b}$ |
| T2 (200ppm) | $7.3^{ab}$ | $13.5^{ab}$ | $20.9^{a}$ | $35.6^{a}$ | $51.9^{a}$ | $58.1^{ab}$ | $69.5^{ab}$ | $71.5^{ab}$ |
| T3 (100ppm + FOL) | $6.3^{cd}$ | $13.2^{ab}$ | $19.3^{ab}$ | $33.3^{a}$ | $45.1^{bc}$ | $54.6^{b}$ | $63.1^{ab}$ | $65.1^{ab}$ |
| T4 (100ppm) | $6.5^{bcd}$ | $13.9^{a}$ | $18.6^{ab}$ | $33.0^{a}$ | $44.1^{bc}$ | $52.6^{b}$ | $60.8^{b}$ | $62.8^{b}$ |
| T5 (fungicide + FOL) | $6.3^{cd}$ | $14.1^{a}$ | $21.6^{a}$ | $34.3^{a}$ | $50.8^{abc}$ | $69.1^{a}$ | $71.1^{ab}$ | $73.1^{ab}$ |
| T6 (loquat extract + FOL) | $6.6^{bcd}$ | $14.3^{a}$ | $22.6^{a}$ | $36.7^{a}$ | $55.6^{a}$ | $70.2^{a}$ | $75.2^{a}$ | $77.2^{a}$ |
| T7 (FOL-only control) | $5.3^{d}$ | $12^{ab}$ | $19.3^{ab}$ | $32.8^{a}$ | $46.7^{bc}$ | $56.9^{ab}$ | $62.7^{ab}$ | $64.7^{ab}$ |
| T8 (healthy control) | $7.6^{a}$ | $13.3^{ab}$ | $22.1^{a}$ | $35.2^{a}$ | $48.9^{abc}$ | $59.1^{ab}$ | $62.9^{ab}$ | $64.9^{ab}$ |

Means followed by a different letter(s) in the same column differ significantly according to Fisher's least significant difference test (LSD); *Plant heights were determined based on 10 replicates of each treatment.

As the experiment progressed, the suppressive impact of high AgNP concentration became more evident. By week 7, T1 recorded the lowest plant height among all treatments, reinforcing the hypothesis that prolonged exposure to 200ppm AgNPs in the presence of FOL impairs vegetative development. In contrast, T6 consistently demonstrated superior growth from week 9 onward, suggesting a potential biostimulant effect of loquat leaf extract. By weeks 13 and 15, growth trends stabilized, with T6 maintaining the highest average plant height, while T1 remained among the least vigorous. Notably, FOL infection alone (T7) did not significantly reduce plant height, which supports findings by Ansari et al. (2012), who observed limited impact of FOL on tomato growth parameters compared to *Meloidogyne incognita* race 2. These observations highlight the importance of optimizing AgNP concentrations and exploring natural extracts such as loquat for sustainable disease management and growth enhancement. Additionally, Alidoust and Isoda (2014) observed similar growth inhibition in rice shoots treated with γ-$Fe_2O_3$ nanoparticles, supporting the hypothesis that certain nanoparticles can negatively affect plant development. Treatments T5 (fungicide + FOL) and T6 (loquat extract + FOL) demonstrated superior performance, likely due to their protective and nutritive properties, respectively.

Table 3 summarizes the stem diameter and shoot fresh weight measurements across various treatments. Stem diameter showed no statistically significant differences among treatments, except for T7 (FOL-only control), which recorded the lowest mean value when compared to T5 (fungicide + FOL), T6 (loquat extract + FOL) and T8 (healthy control). The highest stem diameter was observed in T8, with significant differences noted between T8, T7 and T3 (100ppm AgNPs + FOL). These findings suggest that higher

**Table 3:** Effect of AgNPs treatments on plant growth parameters of tomato cv. Dafnes, grown under greenhouse conditions

| Treatment | Plant growth parameters* | | | | |
|---|---|---|---|---|---|
| | Stem diameter (mm) | Shoot fresh weight (gm) | Shoot dry weight (gm) | Root fresh weight (gm) | Root dry weight (gm) |
| T1 (200ppm + FOL) | $5.3^{abc}$ | $34.2^{dc}$ | $1.9^{e}$ | $1.07^{c}$ | $0.8^{c}$ |
| T2 (200ppm) | $5.5^{abc}$ | $46.1^{abcd}$ | $3.3^{de}$ | $1.0^{c}$ | $0.7^{c}$ |
| T3 (100ppm + FOL) | $5.1^{bc}$ | $41.7^{bcd}$ | $5.0^{dc}$ | $1.2^{c}$ | $0.8^{c}$ |
| T4 (100ppm) | $5.4^{abc}$ | $48.2^{abc}$ | $8.8^{ab}$ | $2.0^{bc}$ | $1.4^{bc}$ |
| T5 (fungicide + FOL) | $6.0^{ab}$ | $61.0^{a}$ | $10.6^{a}$ | $3.8^{a}$ | $3.3^{a}$ |
| T6 (loquat extract + FOL) | $6.0^{ab}$ | $30.9^{d}$ | $5.7^{cde}$ | $3.6^{ab}$ | $3.2^{a}$ |
| T7 (FOL-only control) | $4.7^{c}$ | $50.2^{a}$ | $6.6^{bc}$ | $2.5^{ab}$ | $2.2^{ab}$ |
| T8 (healthy control) | $6.5^{a}$ | $54.0^{a}$ | $8.1^{a}$ | $3.6^{a}$ | $3.2^{a}$ |

Means followed by a different letter(s) in the same column differ significantly according to Fisher's least significant difference test (LSD). No of replicates (n) = 10 pots/treatment; *Plant growth parameters were determined based on 10 replicates of each treatment.

concentrations of AgNPs did not significantly influence stem diameter. Although T7 exhibited the lowest mean stem diameter (4.7mm), the variation was not statistically significant overall. Regarding shoot fresh weight, the highest mean value was recorded in T5 (fungicide + FOL), which was significantly greater than those in T1 (200ppm AgNPs + FOL), T3 (100ppm AgNPs + FOL) and T6 (loquat extract + FOL), indicating that fungicide application enhanced biomass accumulation. Conversely, T6 showed the lowest shoot fresh weight, with significant differences compared to T4 (100ppm AgNPs), T5, T7 and T8. No significant differences were observed among the remaining treatments.

Analysis of shoot dry weight revealed that tomato plants treated with fungicide (T5; fungicide + FOL) exhibited the highest mean value among all treatments, while the lowest was recorded in T1 (200ppm AgNPs + FOL). The difference was statistically significant between T5 and treatments T1, T2 (200ppm AgNPs), T3 (100ppm AgNPs + FOL), T6 (loquat extract + FOL) and T7 (FOL-only control), as shown in Table 3. These findings suggest that fungicide application was more effective in promoting shoot biomass than treatments involving AgNPs. This observation aligns with the study by Farghaly and Nafady (2015), who reported that biosynthesized AgNPs exerted stress on tomato and wheat plants, resulting in reduced shoot dry weight, which was also evident in the present study. Regarding root biomass, data presented in Table 3 indicate that plants treated with AgNPs (T1 and T3) had the lowest fresh and dry root weights. In contrast, T5 (fungicide + FOL) yielded the highest root biomass, outperforming all other treatments. The diminished root biomass observed in AgNP-treated plants may be attributed to the cytotoxic effects of AgNPs. Sweet and Singleton (2015) reported that high concentrations of AgNPs induced cytotoxicity in pine roots, potentially due to the release of $Ag^{+}$ ions from nanoparticle dissolution. Similarly, Tanti et al. (2012) documented chromosomal aberrations and a decline in mitotic index in *Allium sativum* roots exposed to increasing AgNP concentrations. Conversely, Jung et al. (2010) demonstrated that AgNPs could enhance biomass and dry weight in green onions when used against *Sclerotium cepivorum*, suggesting a context-dependent antifungal efficacy.

The application of green-synthesized AgNPs demonstrated variable effects on the growth and development of tomato plants (cv. Dafnes) under greenhouse conditions. While early-stage treatment with 200ppm AgNPs showed a transient increase in plant height, prolonged exposure particularly in combination with FOL resulted in suppressed growth, reduced shoot and root biomass, and diminished stem diameter. These inhibitory effects are likely attributed to the cytotoxic nature of AgNPs at higher concentrations, as supported by previous studies reporting oxidative stress, chromosomal aberrations and reduced mitotic activity in plant tissues. Among the tested groups, the lowest disease incidence was observed in T5 (fungicide + FOL), where only 5 out of 10 plants exhibited symptoms, corresponding to a 50% incidence rate and a severity score of 2.0. In contrast, treatments T6 (loquat extract + FOL) and T7 (FOL-only control) both resulted in 100% disease incidence, with all plants showing symptoms and a severity score of 2.0. Silver nanoparticle treatments showed moderate efficacy. T1 (200ppm AgNPs + FOL) resulted in a 70% disease incidence, while T3 (100ppm AgNPs + FOL) showed an 80% incidence. Both treatments had a lower severity score of 1.0, indicating that although symptoms were present, the intensity of infection was milder compared to other treatments. Overall, the data suggests that while green-synthesized AgNPs may reduce disease severity, they are less effective than conventional fungicides in preventing infection.

The findings of this study support the potential of biosynthesized AgNPs as effective agents in suppressing FOL, the causal agent of vascular wilt in tomato. The use of plant-mediated AgNPs, particularly those synthesized from *Eriobotrya japonica*, demonstrated significant antifungal activity both in vitro and under greenhouse conditions. These results align with recent studies showing that green-synthesized AgNPs can inhibit FOL and enhance plant defense responses (Ahmad et al. 2022; El-Wafai et al. 2025). Compared to conventional fungicides, AgNPs offer a more sustainable and environmentally friendly alternative, with reduced risk of resistance development and minimal phytotoxicity (Shahid et al. 2023; Dávila Costa & Romero, 2025). Moreover, the comparative efficacy of AgNPs synthesized from different plant extracts highlights the importance of phytochemical composition in nanoparticle performance, as previously reported by Ashraf et al. (2025). The integration of green nanotechnology into plant protection strategies not only addresses the limitations of chemical control but also contributes to the development of resilient crop systems, particularly in regions vulnerable to soil-borne pathogens such as the Jordan Valley.

## Conclusion

In this study, AgNPs were successfully synthesized via a one-step green synthesis method using *Eriobotrya japonica* (loquat) leaf extract. The biosynthesis process yielded

spherical AgNPs, which were thoroughly characterized using XRD, UV–Vis, SEM and EDS. SEM and XRD analyses confirmed the spherical morphology and particle size distribution ranging from 8 to 20nm. The crystalline structure and elemental composition of the nanoparticles were further validated through EDS analysis. The synthesized AgNPs exhibited notable antifungal activity against FOL, a major plant pathogenic fungus. These findings suggest that green-synthesized AgNPs derived from silver nitrate and plant extracts hold promise as eco-friendly antifungal agents with potential applications in agricultural disease management. However, the study also revealed that elevated concentrations of AgNPs may exert phytotoxic effects, particularly when applied to tomato plants over extended periods. This limits their effectiveness as a standalone treatment for Fusarium wilt. Therefore, future research should aim to optimize nanoparticle concentrations and investigate synergistic formulations with biocompatible agents or natural extracts to optimize antifungal effectiveness while reducing phytotoxic impacts on plant health.

## DECLARATIONS

**Funding:** The authors acknowledge funding from the Dean ship of the Scientific Research, the University of Jordan.

**Acknowledgement:** The authors would like to express their sincere gratitude to the University of Jordan for providing the necessary facilities, equipment, and access to the greenhouse that enabled the successful execution of this experiment.

**Conflict of Interest:** None.

**Data Availability:** All the data is available in the article.

**Ethics Statement:** This article does not involve studies with human participants or animals; therefore, ethical approval was not required.

**Author's Contribution:** Nida Salem: Conceptualization; supervision of in vitro and in planta experiments; writing, editing and reviewing the paper. Akel Awad: Conceptualization; nanoparticle synthesis design and supervision; writing and editing. Rebhi Darwazeh: Experimental investigation; writing-original draft preparation.

**Generative AI Statement:** The authors declare that no Gen AI/DeepSeek was used in the writing/creation of this manuscript.

**Publisher's Note:** All claims stated in this article are exclusively those of the authors and do not necessarily represent those of their affiliated organizations or those of the publisher, the editors, and the reviewers. Any product that may be evaluated/assessed in this article or claimed by its manufacturer is not guaranteed or endorsed by the publisher/editors.

## REFERENCES

Abkhoo, J., & Panjehkeh, N. (2016). Evaluation of antifungal activity of silver nanoparticles on *Fusarium oxysporum*. *International Journal of Infection, 4*, e41126. https://doi.org/10.5812/iji.41126

Aguilar-Mendez, M.A., Martin-Martinez, E.S., Ortega-Arroyo, L., Cobiab-Portillo, G., & Sanchez-Espindola, E. (2011). Synthesis and characterization of silver nanoparticles: Effect on phytopathogen *Colletotrichum gloesporioides*. *Journal of Nanoparticle Research, 13*, 2525–2532. https://doi.org/10.1007/s11051-010-0145-6

Ahmad, M., Ali, A., Ullah, Z., Sher, H., Dai, DQ., Ali, M., Iqbal, J., Zahoor, M., & Ali, I. (2022). Biosynthesis of silver nanoparticles using *Polygonatum geminiflorum* and their antifungal activity against *Fusarium oxysporum*. *Frontiers in Bioengineering and Biotechnology, 10*, 988607. https://doi.org/10.3389/fbioe.2022.988607

Alidoust, D., & Isoda, A. (2014). Phytotoxicity assessment of γ-$Fe_2O_3$ nanoparticles on root elongation and growth of rice plant. *Environmental Earth Sciences, 71*(12), 5173–5182. https://doi.org/10.1007/s12665-013-2920-z

Al-Khatib, M., Abu-Blan, H., & Masoud, S. (2004). Determination of resistance of locally grown tomato varieties to *Fusarium oxysporum* f. sp. *lycopersici* in Jordan under greenhouse conditions. *Jordan Journal of Agricultural Sciences, 6*(1), 1–10.

Ansari, S., Shahab, S., Mazid, M., & Ahmed, D. (2012). Comparative study of *Fusarium oxysporum* f. sp. *lycopersici* and *Meloidogyne incognita* race-2 on plant growth parameters of tomato. *Agricultural Sciences, 3*(6), 844–847. https://doi.org/10.4236/as.2012.36102

Arabyat, S. (2004). *Effect of treated wastewater on Fusarium wilt of tomato and stalk rot of sweet corn and host resistance* (PhD thesis). Faculty of Agriculture, University of Jordan, Amman, Jordan.

Ashraf, M., Khan, M.A., & Ali, S. (2025). Phytofabricated silver nanoparticles from *Pongamia pinnata* for *Fusarium* wilt management in tomato. *Scientific Reports, 15*(1), 89724. https://doi.org/10.1038/s41598-025-89724-4

Awwad, A.M., Salem, N.M., & Abdeen, A.O. (2013). Green synthesis of silver nanoparticles using carob leaf extract and its antibacterial activity. *International Journal of Industrial Chemistry, 4*(1), 1–6. https://doi.org/10.1186/2228-5547-4-29

Awwad, A.M., Salem, N.M., & Ibrahim, Q.M. (2016). Rapid and large-scale green synthesis of silver nanoparticles using *A. altissima* leaves extract. *Arab Journal of Physical Chemistry, 3*, 17–21.

Baskar, V., Venkatesh, J., & Park, S.W. (2015). Impact of biologically synthesized silver nanoparticles on the growth and physiological responses of *Brassica rapa* ssp. *pekinensis*. *Environmental Science and Pollution Research, 22*(22), 17672–17682. https://doi.org/10.1007/s11356-015-4864-1

Cakır, B., Gül, A., Yolageldi, L., & Özaktan, H. (2014). Response to *Fusarium oxysporum* f. sp. *radicis-lycopersici* in tomato roots involves regulation of SA- and ET-responsive gene expressions. *European Journal of Plant Pathology, 139*(2), 379–391. https://doi.org/10.1007/s10658-014-0394-9

Choudhary, S., Bagri, R.K., Chaurasiya, D.K., Ghasolia, R.P., & Yadav, R. (2023). Integrated management strategy of Fusarium wilt of tomato through plant extracts, bio-control agents and fungicides. *Zenodo*. https://doi.org/10.5281/zenodo.7783934

Choudhury, S.R., Ghosh, M., Mandal, A., Chakravorty, D., Pal, M., Pradhan, S., & Goswami, A. (2011). Surface-modified sulfur nanoparticles: An effective antifungal agent against *Aspergillus niger* and *Fusarium oxysporum*. *Applied Microbiology and Biotechnology, 90*(2), 733–743. https://doi.org/10.1007/s00253-011-3142-5

Das, R.K., Brar, S.K., & Verma, M. (2015). Effects of different metallic nanoparticles on germination and morphology of *Rhizopus oryzae* 1526 and changes in the production of fumaric acid. *BioNanoScience, 5*(4), 1–10. https://doi.org/10.1007/s12668-015-0183-8

Dávila Costa, J.S., & Romero, A.M. (2025). Nano-biofungicides: A sustainable approach to plant disease management. *Biophysica, 5*(2), 15. https://doi.org/10.3390/biophysica5020015

Devi, J.S., & Bhimba, B.V. (2014). Antibacterial and antifungal activity of silver nanoparticles synthesized using *Hypnea muciformis*. *Biosciences Biotechnology Research Asia, 11*, 235–238. https://doi.org/10.13005/bbra/1260

Eker, F., Akdaşçi, E., Duman, H., Bechelany, M., & Karav, S. (2025). Green synthesis of silver nanoparticles using plant extracts: A comprehensive review of physicochemical properties and multifunctional applications. *International Journal of Molecular Sciences, 26*(13), 6222. https://doi.org/10.3390/ijms26136222

El-Wafai, N., El-Mougy, N., & Abdel-Kader, M. (2025). Biogenic silver

nanoparticles for controlling Fusarium wilt in tomato. *Journal of Plant Pathology, 107*(2), 1948–1959. https://doi.org/10.1007/s42161-025-01948-5

Farghaly, F.A., & Nafady, N.A. (2015). Green synthesis of silver nanoparticles using leaf extract of *Rosmarinus officinalis* and its effect on tomato and wheat plants. *Journal of Agricultural Science, 7*(11), 277–287. https://doi.org/10.5539/jas.v7n11p277

Gopinath, V., & Velusamy, P. (2013). Extracellular biosynthesis of silver nanoparticles using *Bacillus* sp. GP-23 and evaluation of their antifungal activity towards *Fusarium oxysporum*. *Spectrochimica Acta Part A: Molecular and Biomolecular Spectroscopy, 106*, 170–174. https://doi.org/10.1016/j.saa.2012.12.087

Hamaideh, A., Al-Zghoul, T., Dababseh, N., & Jamrah, A. (2024). Enhancing water management in Jordan: A fresh tomato water footprint analysis. *Jordan Journal of Agricultural Sciences, 20*(4), 276–294. https://doi.org/10.35516/jjas.v20i4.2571

Haruna, S.G., Yahuza, L., & Tijjani, I. (2024). Management of *Fusarium* wilt of tomato (*Fusarium oxysporum* f. sp. *lycopersici*) using eco-friendly methods: A review. *Asian Journal of Research in Crop Science, 9*(1), 154–168. https://doi.org/10.9734/ajrcs/2024/v9i1257

Hassan, H.A. (2020). Biology and integrated control of tomato wilt caused by *Fusarium oxysporum lycopersici*: A comprehensive review. *Journal of Botany Research, 3*(1), 1–20. https://doi.org/10.36959/771/565

Heikal, Y.M., Albahi, A.M., Alyamani, A.A., Abdelmigid, H.M., Haroun, S.A., & Soliman, H.M. (2025). Integrated management of tomato Fusarium wilt: Ultrastructure insights into Zn nanoparticles and phytohormone applications. *Cells, 14*(14), 1055. https://doi.org/10.3390/cells14141055

Jorge, P.E., Green, R.J., & Chaney, R. (1992). Inoculation with *Fusarium* and *Verticillium* to increase resistance in Fusarium-resistant tomato. *Plant Disease, 76*(4), 340–343.

Jung, J.H., Kim, S.W., Min, J.S., Kim, Y.J., Lamsal, K., Kim, K.S., & Lee, Y.S. (2010). The effect of nano-silver liquid against the white rot of green onion caused by *Sclerotium cepivorum*. *Mycobiology, 38*(1), 39–45. https://doi.org/10.4489/MYCO.2010.38.1.039

Kanhed, P., Birla, S., Gaikwad, S., Gade, A., Seabra, A.B., Rubilar, O., & Rai, M. (2014). In vitro antifungal efficacy of copper nanoparticles against selected crop pathogenic fungi. *Materials Letters, 115*, 13–17. https://doi.org/10.1016/j.matlet.2013.10.011

Khatami, M., Pourseyedi, S., Khatami, M., Hamidi, H., Zaeifi, M., & Soltani, L. (2015). Synthesis of silver nanoparticles using seed exudates of *Sinapis arvensis* and evaluation of their antifungal activity. *Bioresources and Bioprocessing, 2*(1), 1–7. https://doi.org/10.1186/s40643-015-0043-y

Kim, S.W., Jung, J.H., Lamsal, K., Kim, Y.S., Min, J.S., & Lee, Y.S. (2012). Antifungal effects of silver nanoparticles against various plant pathogenic fungi. *Mycobiology, 40*(1), 53–58. https://doi.org/10.5941/MYCO.2012.40.1.053

Kim, S.W., Kim, K.S., Lamsal, K., Kim, Y.J., Kim, S.B., Jung, M., Sim, S.J., Kim, H.S., Chang, S.J., Kim, J.K., & Lee, Y.S. (2009). In vitro antifungal effect of silver nanoparticles on oak wilt pathogen *Raffaelea* sp. *Journal of Microbial Biotechnology, 19*(8), 760–764. https://doi.org/10.4014/jmb.0812.649

Lamsal, K., Kim, S., Jung, J.H., Kim, Y.S., Kim, K.S., & Lee, Y.S. (2011). Inhibition effects of silver nanoparticles against powdery mildews on cucumber and pumpkin. *Mycobiology, 39*(1), 26–32. https://doi.org/10.4489/MYCO.2011.39.1.026

Leslie, J.F., & Summerell, B.A. (2006). *The Fusarium laboratory manual* (1st ed.). Blackwell Publishing. https://doi.org/10.1002/9780470278376

Mahdizadeh, V., Safaie, N., & Khelghatibana, F. (2015). Evaluation of antifungal activity of silver nanoparticles against some phytopathogenic fungi and *Trichoderma harzianum*. *Journal of Crop Protection, 4*, 291–300. https://doi.org/10.48311/jcp.2015.1214

Mazhar, S., Hyder, S., Khan, B.S., Gondal, A.S., Ahmed, R., & Iqbal, M. (2025). Green synthesis of silver nanoparticles using guava leaves: An effective strategy to control chili fruit rot disease. *BMC Plant Biology, 25*, Article 499. https://doi.org/10.1186/s12870-025-06528-4

Medda, S., Hajra, A., Dey, U., Bose, P., & Mondal, N.K. (2014). Biosynthesis of silver nanoparticles from *Aloe vera* leaf extract and antifungal activity against *Rhizopus* sp. and *Aspergillus* sp. *Applied Nanoscience*, 1–6. https://doi.org/10.1007/s13204-014-0387-1

Miller, S.A., Rowe, R.C., & Riedel, R.M. (1986). *Fusarium and Verticillium wilts of tomato, potato, pepper, and eggplant* (Extension Factsheet Hyg-3122-96). The Ohio State University.

Narayanan, K.B., & Park, H.H. (2014). Antifungal activity of silver nanoparticles synthesized using turnip leaf extract (*Brassica rapa* L.) against wood rotting pathogens. *European Journal of Plant Pathology, 140*(2), 185–192. https://doi.org/10.1007/s10658-014-0399-4

O'Donnell, K., Kistler, H.C., Cigelnik, E., & Ploetz, R.C. (1998). Multiple evolutionary origins of the fungus causing Panama disease of banana. *Proceedings of the National Academy of Sciences, 95*(5), 2044–2049. https://doi.org/10.1073/pnas.95.5.2044

Pandey, A.K., Dinesh, K., Nirmala, N.S., & Dutta, P. (2024). *Fusarium wilt of tomato: Past, present, and future*. In *Plant pathogen interaction* (pp. 55–87). Springer. https://doi.org/10.1007/978-981-99-4890-1_3

Shahid, M., Irshad, M., & Khan, M. (2023). Green nanoparticles as alternatives to chemical fungicides: A review. *Agrobiological Records, 14*, 59–69. https://doi.org/10.5281/zenodo.10415235

Steinkellner, S., Mammerler, R., & Vieheilig, H. (2008). Germination of *Fusarium oxysporum* in root exudates from tomato plants challenged with different *F. oxysporum* strains. *European Journal of Plant Pathology, 122*(3), 395–401. https://doi.org/10.1007/s10658-008-9306-1

Sweet, M.J., & Singleton, I. (2015). Soil contamination with silver nanoparticles reduces Bishop Pine growth and ectomycorrhizal diversity on pine roots. *Journal of Nanoparticle Research, 17*, 488. https://doi.org/10.1007/s11051-015-3246-4

Tabassum, R.Z., Mehmood, A., Khalid, A.R., Ahmad, K.S., Khan, M.A.R., Amjad, M.S., Raffi, M., Khan, G., & Mustafa, A. (2024). Green synthesis of silver nanoparticles for antifungal activity against tomato Fusarium wilt caused by *Fusarium oxysporum*. *Biocatalysis and Agricultural Biotechnology, 61*, 103376. https://doi.org/10.1016/j.bcab.2024.103376

Tanti, B., Das, A.K., Kakati, H., & Chowdhury, D. (2012). Cytotoxic effect of silver nanoparticles on root meristem of *Allium sativum* L. *Journal of Research in Nanobiotechnology, 1*(1), 1–8.

Vanlalveni, C., Lallianrawna, S., Biswas, A., Selvaraj, M., Changmai, B., & Rokhum, S.L. (2021). Green synthesis of silver nanoparticles using plant extracts and their antimicrobial activities: A review. *RSC Advances, 11*(5), 2804–2823. https://doi.org/10.1039/D0RA09941D

Venkatesham, M., Ayodhya, D., Madhusudhan, A., Kumari, A.S., Veerabhadram, G., & Mangatayaru, K.G. (2014). A novel green synthesis of silver nanoparticles using gum karaya. *Journal of Cluster Science, 25*, 409–422. https://doi.org/10.1007/s10876-013-0620-1

Wang, L.S., Wang, C.Y., Yang, C.H., Hsieh, C.L., Chen, S.Y., Shen, C.Y., Wang, J.J., & Huang, K.S. (2015). Synthesis and antifungal effect of silver nanoparticles–chitosan composite particles. *International Journal of Nanomedicine, 10*, 2685–2696. https://doi.org/10.2147/IJN.S77410

White, T.J., Lee, S., & Taylor, J. (1990). PCR protocols: A guide to methods and applications. In M. A. Innis, D. H. Gelfand, J. J. Sninsky, & T. J. White (Eds.), *PCR protocols* (pp. 315–322). Academic Press.

Yehia, R.S., & Ahmed, O.F. (2013). In vitro study of the antifungal efficacy of zinc oxide nanoparticles against *Fusarium oxysporum* and *Penicillium expansum*. *African Journal of Microbiology Research, 7*(19), 1917–1923. https://doi.org/10.5897/AJMR2013.5668